# Timing of Neoproterozoic glaciations linked to transport-limited global weathering

Benjamin Mills[1*], Andrew J. Watson[1], Colin Goldblatt[2], Richard Boyle[3] & Timothy M. Lenton[3]

[1]*School of Environmental Sciences, University of East Anglia, Norwich, NR4 7TJ, U.K.*

[2]*School of Earth and Ocean Sciences, University of Victoria, PO Box 3065 STN CS, Victoria, British Columbia, V8W 3V6, Canada.*

[3]*College of Life and Environmental Sciences, University of Exeter, Exeter EX4 4PS, UK, previously at School of Environmental Sciences, University of East Anglia, Norwich, NR4 7TJ, U.K.*

**The Earth underwent several snowball glaciations between 1,000 and 542 Myr ago. The termination of these glaciations is thought to have been triggered by the accumulation of volcanic $CO_2$ in the atmosphere over millions of years [1,2]. Subsequent high temperatures and loss of continental ice would increase silicate weathering and in turn draw down atmospheric $CO_2$ [3]. Estimates of the post-snowball weathering rate indicate that equilibrium between $CO_2$ input and removal would be restored within several million years [4], triggering a new glaciation. However the transition between deglaciation and the onset a new glaciation was on the order of $10^7$ years. Over long timescales, the availability of fresh rock can become a limiting factor for silicate weathering rates [5]. Here we show that when this limitation is incorporated into the COPSE biogeochemical model [6], the stabilization time is substantially higher, $>10^7$ years. When we include a simple ice albedo feedback, the model produces greenhouse-icehouse oscillations on this timescale that are compatible with observations. Our simulations also indicate positive carbon isotope excursions and an increased flux of oxygen to the atmosphere during interglacials, both of which are consistent with the geological record [7,8]. We conclude that the long gaps between snowball glaciations can be explained by limitations on silicate weathering rates.**

The Neoproterozoic era (1000-542Ma) is punctuated by at least three glaciations [9], the severe low-latitude Sturtian and Marinoan episodes being proposed as examples of `Snowball Earth' events [1, 10]. Figure 1 displays Neoproterozoic carbonate carbon isotope data [7], which shows a quasi-periodic pattern. Negative excursions associated with glaciation appear at ~50 Myr intervals between long periods of positive fractionation. The long interval between glaciations poses a puzzle given the standard model of a snowball Earth being terminated by very high $CO_2$ and temperature. The time taken to restore equilibrium after such a perturbation depends on the rate of $CO_2$ drawdown via silicate weathering, a process that would be greatly enhanced in the aftermath of snowball Earth. Highly weatherable rock flour produced by glacial grinding would likely cover a large surface area, and increased temperature and runoff should allow for an elevated weathering flux. Linked GCM and kinetic weathering models have determined the maximum weathering rate in this climate to be on the order of 10 times the modern day flux, implying a timescale of around $10^6$ years to reduce atmospheric $CO_2$ to pre-glacial levels [4]. Based on these results, we would expect the system to establish equilibrium in a time far shorter than the interglacial periods following the Sturtian and Marinoan glaciations.

Here we propose that the timescale for $CO_2$ drawdown following a snowball glaciation should be extended due to transport limitation of the silicate weathering process. In a transport limited regime, silicate cations are completely leached from fresh regolith and therefore the rate of chemical weathering depends only on the physical erosion rate [5]. Modern continental cratons are transport limited, as seen by plotting the rate of denudation of silicate cations against total denudation rate [11]. In such a regime, increasing temperature or runoff does not increase the rate of $CO_2$ drawdown, because all the available silicate cations are already being processed. As global temperature and humidity rises, we would expect more weathering zones to become transport-limited, implying a theoretical maximum silicate weathering rate, where every available cation is leached.

Over the Phanerozoic, the mean continental erosion rate is estimated to be ~16m $Myr^{-1}$ [12]. Using the average density and area of the present day continents (area=$1.5 \times 10^{14}$ $m^2$, density = $2.5 \times 10^3$ kg $m^{-3}$) yields a total mass of $6 \times 10^{12}$ kg $yr^{-1}$. Assuming a cation weight fraction of 0.08 [5], we estimate a global silicate weathering rate maximum for the Phanerozoic of around $4.8 \times 10^{11}$ kg $yr^{-1}$. This maximum transport limited rate is about 2.4 times greater than present day weathering rate [13].

Determining the global erosion rate in the Neoproterozoic is difficult, because it depends on the continental area and rate of uplift. Current estimates for Neoproterozoic uplift rates are close to present day values [14], and the majority of studies agree that the total continental area was probably less than it is now. Proxies for global denudation show very low values (<10m $Myr^{-1}$) for the early Phanerozoic, but are likely to be affected by sampling artefacts [15]. The rate of volcanic degassing in the Neoproterozoic is also important, as it is the balance between $CO_2$ degassing and its consumption rate via weathering and burial that dictates the system response time to large perturbations. In carbon cycle models, degassing is usually assumed to be proportional to the seafloor spreading rate. Accounting for different continental growth models, the Neoproterozoic outgassing rate was probably between 1 and 5 times the present day rate [14, 16]. But smaller crustal carbon content in the Neoproterozoic [17] may have decreased the $CO_2$ content of volcanic gas by up to 20%.

In figure 2, we use a modified version of the COPSE biogeochemical model [6] (see supplementary information) to investigate the effect of a weathering rate cap on the time taken to return to steady state after the suggested snowball exit concentration of 0.3 atm $CO_2$ [1, 2] is imposed. Silicate weathering rate is fixed at a prescribed maximum value, $W_{max}$, which is defined relative to the present day rate. We find that choice of $W_{max}$ has a strong effect on the system: Assuming the Phanerozoic average erosion rate ($W_{max}$=2.4) yields a stabilisation time of ~$10^7$ years, even for conservative estimates of the $CO_2$ degassing rate *D*. A lower erosion rate, and/or a higher degassing rate increases the stabilisation time greatly. For further model runs we let global weathering follow a simple kinetic equation as described by Berner [18], but asymptote to $W_{max}$ as the kinetic weathering rate approaches the transport-limited value, placing a cap on global weathering rates. The choice of kinetic weathering function, and the nature of the transition to $W_{max}$ has negligible effect on results as the rate remains at $W_{max}$ until $CO_2$ is very close to the stable level.

An important consideration for this work is weathering of rock flour left on the surface after a snowball glaciation, which would be expected to increase weathering kinetics as in the quaternary glacial cycle [19]. Global weathering fluxes would not become limited by transport of fresh rock until the flour produced during the glaciation had been completely leached. Le Hir et al [4] assume a thin soil profile following a snowball, due to evidence of persistent weathering during glaciation [20]. Following their estimate of a 25cm reactive upper layer, we derive a weatherable equivalent of ~$10^{17}$ moles C (see supplementary information).

Figure 3 shows model sensitivity to the initial quantity of rock flour. Here we allow a global weathering rate of 10 times present day when rock flour is present [4], switching to the transport limited equation once a specified amount of carbon has been buried, analogous to the abundance of glacial flour. We find that a weatherable equivalent on the order of $10^{20}$ moles C is required to significantly affect stabilisation time; we use a increased reactive layer depth of 2.5m ($10^{18}$ mol C equiv.) for future model runs, due to uncertainty in estimation.

Our results indicate that the sequence of deep glaciations in the Neoproterozoic could be the result of a change of state in the long-term carbon-climate system to a regime which exhibits self-sustaining oscillations. If there was a long period in which global steady state temperature remained below the value required to trigger a snowball glaciation, this would be manifest as an oscillatory regime, with snowball glaciations alternating with warm phases. Such a temperature forcing may well be attributed to the continental configuration at this time. It has been shown that the position of the continents at low latitudes at 750Ma, along with the prevalence of basaltic lithologies, could provide the necessary cooling to trigger the first snowball event [21]. It is thought that the continents would have remained near low latitudes until 600Ma [22], after which they begin to drift to higher latitudes, relaxing the forcing.

To investigate this possible mechanism we parameterise a runaway ice-albedo feedback in our model by imposing a change in albedo when temperature falls below a given value $T_{crit,}$. Assuming the classic snowball scenario [23], we choose $T_{crit,}$ = 283K and allow deglaciation at 263K. Because deglaciation begins in the tropics, it is assumed to occur at lower temperature than is required for the ice sheets to initially advance. Throughout this work we assume a solar constant for 650Ma (1298 $Wm^{-2}$ [24]), broadly representing the timeframe of interest. This allows glaciation at ~150ppm $CO_2$, close to other estimates [21].

We impose the described cooling scenario in the model, adding a parameter ρ to represent enhancement of kinetic weathering. This follows the treatment of vascular plant colonisation in the Phanerozoic COPSE model runs [6], acting as a multiplier on the kinetic weathering rate equation. To trigger oscillations we increase ρ by a factor of three for a period of 150Myrs. The magnitude of this enhancement is roughly analogous to the increase in basaltic surface area and mid-latitude runoff calculated in ref [21]. For present day $CO_2$ degassing rate ($D$ = 1), we require $W_{max}$ = 1.4 to produce a rough analogue of the Neoproterozoic record. This parameter choice is shown in figure 4. Assuming a higher $CO_2$ degassing rate shortens glacial duration and allows for larger values of $W_{max}$ to produce the observed timing, in line with figure 2.

We use output from the CO2SYS model [25] to approximate the atmospheric fraction of total ocean and atmosphere $CO_2$, assuming that there is gas exchange between atmosphere and ocean during glaciation [1]. The total solubility of $CO_2$ is higher in cold water than warm water, therefore deglaciation causes a large transfer of $CO_2$ from ocean to atmosphere.

The solid line for $\delta^{13}C$ shows the isotopic fractionation of marine carbonates, assuming the fractionation effect on burial takes into account the equilibrium fractionation between oceanic and atmospheric carbon, and a dependence on temperature, as in the full COPSE model [6]. The dashed line shows an alternative solution where fractionation effects are constant. Both treatments yield a continued positive fractionation during the interglacial period due to elevated burial of light organic carbon, due in turn to sustained above-average nutrient fluxes from weathering. Higher assumption of $W_{max}$ increases nutrient delivery and therefore also increases fractionation. Low productivity during glaciations causes a negative excursion. We do not expect a simple model such as this to replicate exactly the isotope record. Negative excursions preceding glaciation are not reproduced by our model, and may be due to direct temperature effects on productivity, which are not included. Our aim is to demonstrate that the extended period of system disequilibrium following a snowball glaciation should contribute to prolonged positive excursions in $\delta^{13}C$, and more complex analysis is required to fully understand the Neoproterozoic carbon cycle.

With the imposition of a suitable long term maximum weathering rate, oscillations in this simple carbon – climate model can provide a qualitative fit to the sequence of glaciations and carbon isotope variations in the Neoproterozoic. The globally transport limited scenario presents a prolonged period of elevated primary productivity, which would support suggested increases in oxygen concentration and phosphorous deposition over this time [7, 8, 26-29]. There is evidence for phosphorous deposition after the Marinoan glaciation but not after the Sturtian.

It is important to note that the mechanism we describe relies on a particular interpretation of the Neoproterozoic period, namely the Snowball Earth hypothesis [1, 10]. It is possible that the Neoproterozoic actually contained more frequent smaller glaciations, which would not terminate via a high $CO_2$ 'super greenhouse'. Due to our long timeframe for $CO_2$ drawdown, our prediction is highly testable, with for example one recent study proposing a rapid decline in $CO_2$ following the

Marinoan glaciation [30]. Further work to establish the duration of any post-glacial greenhouse may thus enable validation or falsification of mechanisms to explain these fascinating events.

## References


1. Hoffman, P.F., Kaufman, A.J., Halverson, G.P., & Schrag, D.P. A Neoproterozoic Snowball Earth. *Science* **281,** 1342-1346 (1998).
2. Pierrehumbert, R.T. Climate dynamics of a hard snowball Earth*. J. Geophys. Res.* **110,** D01111 (2005).
3. Walker, J.C.G., Hays, P.B. & Kasting, J.F. A negative feedback mechanism for the long-term stabilization of earth's surface temperature. *J. Geophys. Res.* **86,** 9776-9782 (1981).
4. Le Hir, G. *et al*. The snowball Earth aftermath: Exploring the limits of continental weathering processes. *Earth Planet. Sci. Lett.* **277,** 453-463 (2009).
5. West, A.J., Galy, A. & Bickle, M. Tectonic and climatic controls on silicate weathering. *Earth Planet. Sci. Lett.* **235,** 211-228 (2005).
6. Bergman, N.M., Lenton, T.M. & Watson, A.J. COPSE: A new model of biogeochemical cycling over phanerozoic time. *Am. J. Sci.* **304,** 397-437 (2004).
7. Halverson, G.P., Hoffman, P.F., Schrag, D.P., Maloof, A.C. & Rice, H.N. Toward a Neoproterozoic composite carbon-isotope record. *Geol. Soc. Amer. Bull.* **117,** 1181-1207 (2005).
8. Canfield, D.E. *et al.* Ferruginous Conditions Dominated Later Neoproterozoic Deep-Water Chemistry. *Science* **321,** 949-952 (2008).
9. Hoffmann, K.-H., Condon, D.J., Bowring, S.A. & Crowley, J.L. U-Pb zircon date from the Neoproterozoic Ghaub Formation, Namibia: Constraints on Marinoan glaciation. *Geology* **32,** 817-820 (2004).
10. Kirschivink, J.L. Late Proterozoic Low-Latitude Global Glaciation: the Snowball Earth. In *The Proterozoic Biosphere: A Multidisciplinary Study* (eds. Schopf, J.W. & Klein, C.) 51-52 (1992).
11. Millot, R., Gaillardet, J., Dupre, B. & Allegre, C.J. The global control of silicate weathering rates and the coupling with physical erosion: new insights from rivers of the Canadian Shield. *Earth Planet. Sci. Lett.* **196,** 83-98 (2002).
12. Wilkinson, B.H. & McElroy, B.J. The impact of humans on continental erosion and sedimentation. *Geol. Soc. Amer. Bull.* **119,** 140-156 (2007).
13. Gaillardet, J., Dupre, B., Louvat, P. & Allegre, C.J. Global silicate weathering and $CO_2$ consumption rates deduced from the chemistry of large rivers. *Chem. Geol.* **159,** 3-30 (1999).
14. Rino, S. *et al.* Major episodic increases of continental crustal growth determined from zircon ages of river sands; implications for mantle overturns in the Early Precambrian. *Phys. Earth Planet. Inter.* **146,** 369-394 (2004).
15. Willenbring, J.K. & Blanckenburg, F.V-. Long-term stability of global erosion rates and weathering during late-Cenozoic cooling. *Nature* **465,** 211-214 (2010).
16. Franck, S. & Bounama, C. Continental growth and volatile exchange during Earth's evolution. *Phys. Earth Planet. Inter.* **100,** 189-196 (1997).
17. Hayes, J.M. & Waldbauer, J.R. The carbon cycle and associated redox processes through time. *Phil. Trans. R. Soc. B* **361,** 931-950 (2006).
18. Berner, R.A. Geocarb II: A revised model of atmospheric $CO_2$ over phanerozoic time. *Am. J. Sci.* **294,** 56-91 (1994).
19. Vance, D., Teagle, D.A.H. & Foster, G.L. Variable Quaternary chemical weathering fluxes and imbalances in marine geochemical budgets. *Nature* **458,** 493-496 (2009).

20. Donnadieu, Y., Fluteau, F., Ramstein, G., Ritz, C. & Besse, J. Is there a conflict between the Neoproterozoic glacial deposits and the snowball Earth interpretation: an improved understanding with numerical modeling. *Earth Planet. Sci. Lett.* **208,** 101-112 (2003).
21. Donnadieu, Y., Godderis, Y., Ramstein, G., Nedelec, A. & Meert, J. A 'snowball Earth' climate triggered by continental break-up through changes in runoff. *Nature* **428,** 303-306 (2004).
22. Li, Z.X. *et al.* Assembly, configuration, and break-up history of Rodinia: A synthesis. *Precamb. Res.* **160,** 179-210 (2008).
23. Hoffman, P.F. & Schrag, D.P. The snowball Earth hypothesis: testing the limits of global change. *Terra Nova* **14,** 129-155 (2002).
24. Caldeira, K. and Kasting, J.F. The life span of the biosphere revisited. *Nature* **360,** 721-723 (1992).
25. Lewis, E. & Wallace, D.W.R. Program developed for $CO_2$ system calculations. *ORNL/CDIAC* **105,** (1998).
26. Shields, G.A. *et al.* Neoproterozoic glaciomarine and cap dolostone facies of the southwestern Taoudeni Basin (Walidiala Valley, Senegal/Guinea, NW Africa). *C. R. Geosci.* **339,** 186-199 (2007).
27. Porter, S.M., Knoll, A.H. & Affaton, P. Chemostratigraphy of Neoproterozoic cap carbonates from the Volta Basin, West Africa. *Precamb. Res.* **130,** 99-112 (2004).
28. Zhu, M., Zhang, J. & Yang, A. Integrated Ediacaran (Sinian) chronostratigraphy of South China. *Palaeogeog. Palaeoclim. Palaeoecol.,* **254** 7-61 (2007).
29. Scott, C. *et al.* Tracing the stepwise oxygenation of the Proterozoic ocean. *Nature* **452,** 456-459 (2008).
30. Kasemann, S.A., Hawkesworth, C.J., Prave, A.R., Fallick, A.E. & Pearson, P.N. Boron and calcium isotope composition in Neoproterozoic carbonate rocks from Namibia: evidence for extreme environmental change. *Earth Planet. Sci. Lett* **231,** 73-86 (2005).

**Corresponding author:**

B.M. is the corresponding author for this work. Email: b.mills@uea.ac.uk

**Acknowledgements:**

BM is funded by a UEA Dean's studentship. AJW's contribution was supported by a Royal Society Research Professorship. Part of CG's contribution was supported by a NASA Postdoctoral Fellowship at Ames Research Center and by the NASA Astrobiology Institute Virtual Planetary Laboratory lead team. AJW, RAB and TML are supported by the NERC project (NE/I005978/1) 'Reinventing the planet: The Neoproterozoic revolution in oxygenation, biogeochemistry and biological complexity'.

**Author Contributions:**

BM and AJW suggested the study. BM wrote the model, results were analysed by BM and AJW. Discussion with CG helped improve the method. RB and TML contributed to the manuscript.

**Competing financial interests statement**

The authors declare that they have no competing financial interests.

**Figure captions**

**Figure 1: $\delta^{13}C$ record for the late Neoproterozoic.** Isotopic composition of carbonates from ref. [7]. The vertical grey bars from left to right denote the Sturtian, Marinoan and Gaskiers glaciations.

**Figure 2: Phase portrait: stabilisation time versus maximum weathering rate, $W_{max}$.** Here we assume an initial $CO_2$ concentration of 0.3 atmospheres, and fix the global weathering rate at $W_{max}$. The three lines show different choices of the relative $CO_2$ degassing rate, $D$. $W_{max}$ is defined relative to present day silicate weathering rate, with the grey vertical line showing our estimate of $W_{max}$= 2.4 for the Phanerozoic. Increasing the weathering rate enhances nutrient delivery and therefore increases the organic burial fraction, allowing stability when $W_{max}$ is somewhat smaller than D, providing $W_{max}$ >1. See supplementary information for full model description.

**Figure 3: Stabilisation time after 0.3 atm $CO_2$ perturbation for different initial abundances of rock flour. a,** Rock flour consumed. **b,** Silicate weathering rate. **c,** Atmospheric $CO_2$ concentration. Here $R_{max}$ denotes the maximum amount of carbon (in moles) that can be drawn down via weathering of glacial rock flour before it is depleted. This figure shows the situation where $D$ = 1, $W_{max}$ = 2.4. The grey vertical line shows the stabilisation time when no flour is present (as in fig2). The second drop in weathering rate here occurs as $CO_2$ returns to a stable concentration.

**Figure 4: Cyclic solution when steady state temperature is forced below the ice-albedo runaway value for 150Myr.** Here we let $D$ = 1 and $W_{max}$ = 1.4 to produce glacial timing on the order observed in the Neoproterozoic. **a,** The imposed kinetic weathering enhancement (ρ) is shown in grey; in black is the weathering rate relative to present. **b,** Total atmosphere/ocean carbon (grey), and atmospheric $CO_2$ (black). **c,** Temperature alongside snowball entry/exit thresholds. **d,** Model $\delta^{13}C$, solid line shows temperature/$CO_2$ dependent fractionation [6], dashed line shows solution when fractionation effects are constant.

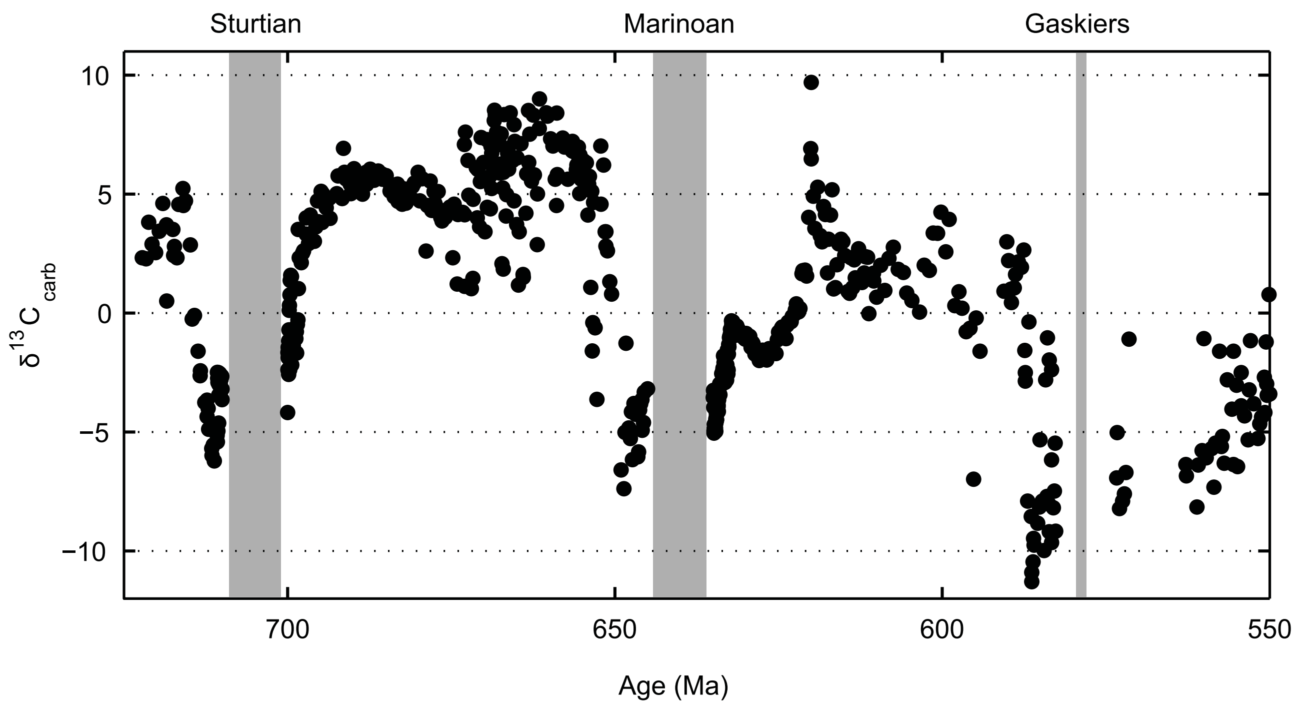

Sturtian
Marinoan
Gaskiers
10
5
0
−5
−10
$\delta^{13}C_{carb}$
700
650
600
550
Age (Ma)

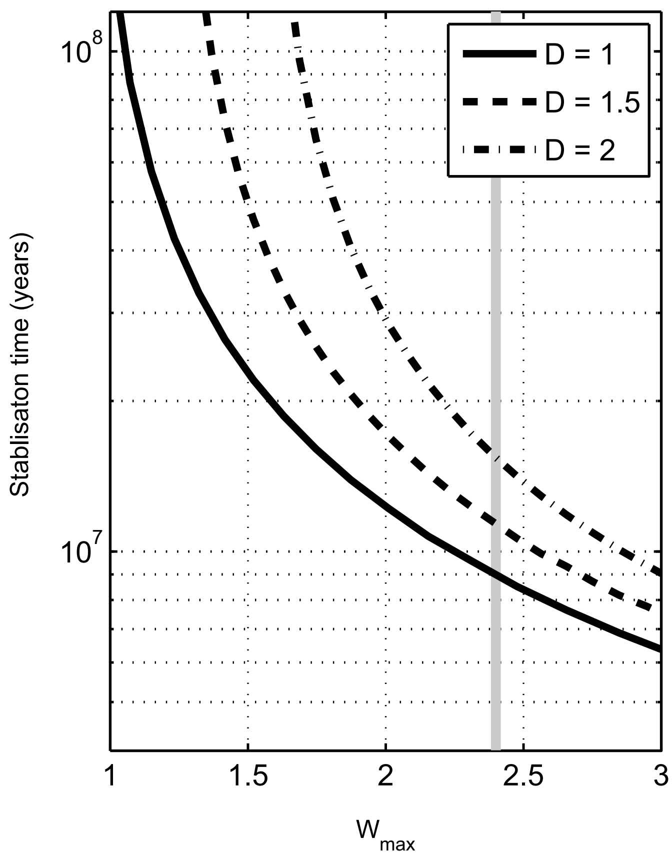

D = 1
D = 1.5
D = 2
Stablisaton time (years)
$10^8$
$10^7$
1
1.5
2
2.5
3
$W_{max}$

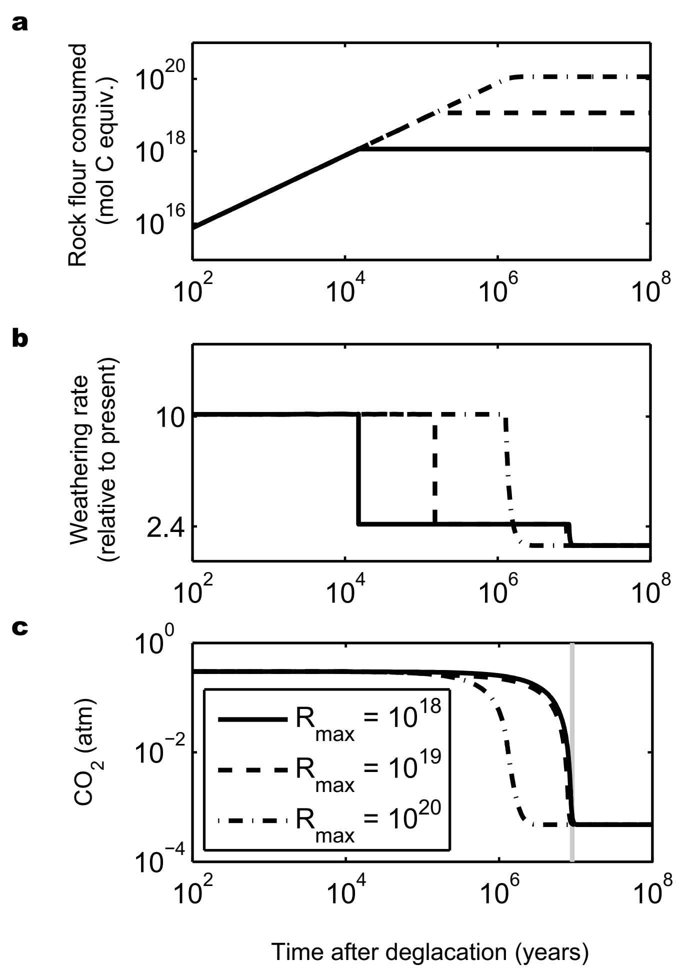
a
Rock flour consumed
(mol C equiv.)
10^20
10^18
10^16
10^2
10^4
10^6
10^8
b
Weathering rate
(relative to present)
10
2.4
10^2
10^4
10^6
10^8
c
10^0
10^-2
10^-4
CO2 (atm)
Rmax = 10^18
Rmax = 10^19
Rmax = 10^20
10^2
10^4
10^6
10^8
Time after deglacation (years)

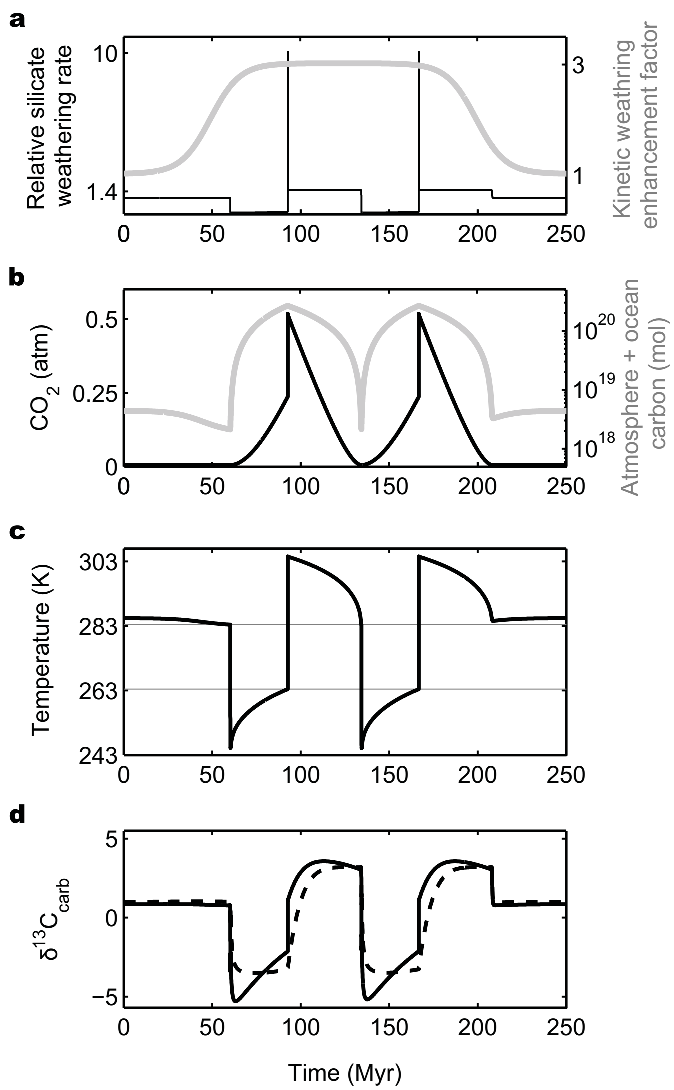
a
Relative silicate weathering rate
Kinetic weathring enhancement factor
10
1.4
3
1
0
50
100
150
200
250
b
CO2 (atm)
Atmosphere + ocean carbon (mol)
0.5
0.25
0
10^20
10^19
10^18
c
Temperature (K)
303
283
263
243
d
δ13Ccarb
5
0
−5
Time (Myr)